2012 American Control Conference
Fairmont Queen Elizabeth, Montréal, Canada
June 27-June 29, 2012

FES based Rehabilitation of the Upper Limb using Input/Output Linearization and ILC

Chris Freeman, Daisy Tong, Katie Meadmore, Ann-Marie Hughes, Eric Rogers and Jane Burridge

Abstract— **To provide effective stroke rehabilitation, a control scheme is developed for upper arm tracking in 3D space using electrical stimulation. In accordance with clinical need, the case where stimulation is applied to two muscles in the arm and shoulder is considered, with the arm supported against gravity by an exoskeletal mechanism. An upper limb model with five degrees of freedom is first developed to represent the unconstrained upper arm, and an input/output linearization controller is applied to decouple the actuated joint angles, and combined with a state-feedback optimal tracking controller. Linear iterative learning controllers are then designed to enforce precise tracking over repeated attempts at the task, and stability conditions for the unactuated joint angles are given. Experimental results confirm practical performance.**

I. INTRODUCTION

Of the 15 million people who annually suffer a stroke worldwide, 5 million are left permanently disabled. Conventional therapy to improve upper limb function following stroke is not effective, and only 5% of survivors with severe paralysis regain upper limb function [1]. During the last decade there has been growing evidence for the effectiveness of technologies including rehabilitation robots [2] and functional electrical stimulation (FES) [3], to reduce impairment post-stroke. Both enable a person with limited physical ability to practice tasks, and the resulting sensory feedback is associated with cortical changes that can bring about recovery of functional movement. Furthermore, FES is motivated by a body of clinical evidence, and theoretical support from neurophysiology and motor learning research showing that the increased degree of functional recovery is closely related to the accuracy with which the stimulation assists the subject's own voluntary completion of a task [4].

Although a wide variety of FES control techniques have been applied for both the lower and upper limbs, few have transferred into clinical practice due to restrictive conditions such as difficulties in obtaining an accurate model, the requirement of minimal set-up time, reduced control over environmental constraints and little possibility of repeating any one test in the program of treatment undertaken. In upper limb patient trials the applied control signal remains mostly open-loop, triggered, or comprises direct application of electromyographic or electroencephalographic signals, after suitable processing, which provide measures of patients' voluntary intention [5]. Closed-loop control of upper limb movement has only rarely transferred to clinical practice, with most cases not using a model of the biomechanical system, favouring artificial neural networks, to create a mapping between muscle activity and joint variables in unimpaired subjects, which is then employed in tests with patients [6]. Limitations include the need for extensive training for each movement performed, and their black-box structure preventing analysis of stability and performance.

Iterative learning control (ILC) is one model-based approach that has been applied in two clinical trials with stroke patients [7]. In the first, FES was applied to the triceps muscle, and ILC updated the stimulation level to assist patients' completion of a planar reaching task [8]. A second system, shown in Fig. 1, was developed to extend the approach to assist 3D movements of the arm with stimulation applied to two muscles in the arm and shoulder. This presented virtual reality tracking tasks to the patient, whose arm was supported by a passive robotic mechanism to provide a safe, productive environment for training across a wide spectrum of patient ability. For each system, clinical trials with stroke patients were conducted involving 18 treatment sessions. These confirmed unparalleled levels of tracking accuracy in both cases, with statistically significant results across a range of outcome measures [9]. The ILC schemes used assumed minor coupling between joints actuated by FES, and could not ensure stability of unactuated joints. This paper addresses these limitations, yielding controllers suitable for widespread application within FES-based stroke rehabilitation.

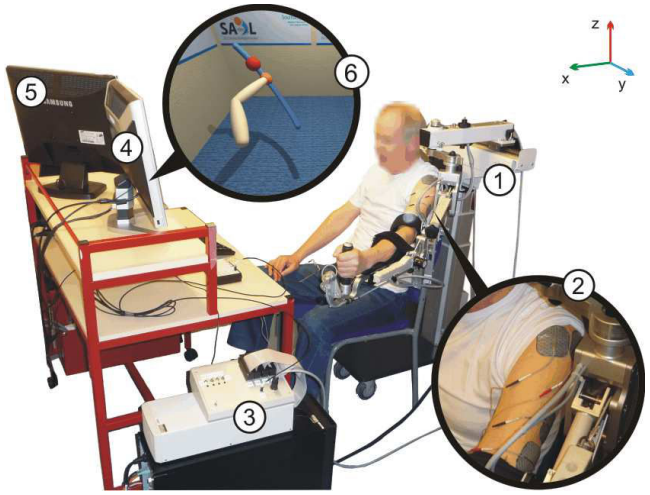

Fig. 1. Rehabilitation system: (1) mechanical support, (2) surface electrodes on triceps and anterior deltoid, (3) realtime processor and interface, (4) monitor displaying task, (5) therapist's monitor and (6) realtime 3D graphics.

C. T. Freeman, D. Tong, K. L. Meadmore and E. Rogers are with the School of Electronics and Computer Science, University of Southampton, SO17 1BJ, UK. A. M. Hughes and J. H. Burridge are with the Faculty of Health Sciences, also at the University of Southampton. cf@ecs.soton.ac.uk.

II. 3D PLATFORM FOR UPPER LIMB FES

A. Mechanical Support

The system shown in Fig. 1 is one of very few to combine robotic therapy and FES, and employs a commercial arm support of a type widely used in stroke rehabilitation. This provides an adjustable force against gravity via two springs incorporated into the mechanism. Each joint is aligned in either the horizontal or vertical plane, as shown in Fig. 2a) which also describes the kinematic structure in terms of the measured the joint variables $\boldsymbol{\Theta} = [\theta_1, \theta_2, \theta_3, \theta_4, \theta_5]^T$. The patient's arm is rigidly strapped to the exoskeleton support.

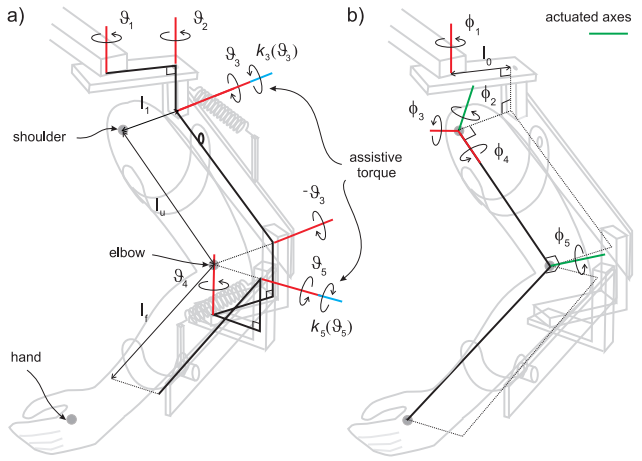

Fig. 2. Kinematic system relationships: a) mechanical support (ArmeoSpring, Hocoma AG) and b) human arm.

B. Muscle Selection and Modelling

Spasticity in stroke patients typically produces a resistance to arm extension associated with overactivity of muscles such as the biceps, wrist and finger flexors, and loss of activity of muscles such as the triceps, anterior deltoid, wrist and finger extensors [10]. Therefore the triceps and anterior deltoid are selected for FES stimulation since they are directly aligned with clinical need. It is first assumed that application of stimulation to the triceps produces a moment about an axis orthogonal to both the forearm and upper arm, and FES to the anterior deltoid produces a moment about an axis which is fixed with respect to the shoulder. The corresponding joint variables (ϕ_5 and ϕ_2 respectively) are shown in Fig. 2b), in which additional joint axes are chosen to encompass the remaining degrees of freedom. A dynamic model of the support which assumes rigid links, is given by

$$\boldsymbol{B}_a(\boldsymbol{\Theta})\ddot{\boldsymbol{\Theta}} + \boldsymbol{C}_a(\boldsymbol{\Theta}, \dot{\boldsymbol{\Theta}})\dot{\boldsymbol{\Theta}} + \boldsymbol{F}_a(\boldsymbol{\Theta}, \dot{\boldsymbol{\Theta}}) + \boldsymbol{G}_a(\boldsymbol{\Theta}) + \boldsymbol{K}_a(\boldsymbol{\Theta}) = 0$$

where $\boldsymbol{B}_a(\cdot)$ and $\boldsymbol{C}_a(\cdot)$ are 5-by-5 inertial and Corelis matrices, and $\boldsymbol{F}_a(\cdot)$ and $\boldsymbol{G}_a(\cdot)$ are friction and gravitational vectors. The vector $\boldsymbol{K}_a(\cdot)$ comprises the moments produced through gravity compensation provided by each spring, which are functions of θ_3 and θ_5 respectively, and hence $\boldsymbol{K}_a(\cdot)$ takes the form $[0, 0, k_3(\theta_3), 0, k_5(\theta_5)]^T$.

Similarly, a dynamic model of the human arm, with FES applied to two muscles, is represented by

$$\boldsymbol{B}_h(\boldsymbol{\Phi})\ddot{\boldsymbol{\Phi}} + \boldsymbol{C}_h(\boldsymbol{\Phi}, \dot{\boldsymbol{\Phi}})\dot{\boldsymbol{\Phi}} + \boldsymbol{F}_h(\boldsymbol{\Phi}, \dot{\boldsymbol{\Phi}}) + \boldsymbol{G}_h(\boldsymbol{\Phi}) = \boldsymbol{\tau}(\boldsymbol{u}, \boldsymbol{\Phi}, \dot{\boldsymbol{\Phi}})$$

in which $\boldsymbol{\tau}(\cdot)$ comprises moments produced through application of FES. Here $\boldsymbol{\Phi} = [\phi_1, \phi_2, \phi_3, \phi_4, \phi_5]^T$ corresponds to anthropomorphic joints, including those actuated by stimulated muscle. As discussed in [11], the most prevalent form of muscle representation is the Hill-type model

$$\tau_i(u_i(t), \phi_i, \dot{\phi}_i) = h_i(u_i, t) \cdot F_{m,i}(\phi_i, \dot{\phi}_i) \qquad i \in \{2, 5\} \quad (1)$$

where $u_2(t)$ and $u_5(t)$ are the FES signals applied to the anterior deltoid and triceps muscles respectively. Here $h_i(u_i, t)$ is a Hammerstein structure with static non-linearity, $h_{IRC,i}(u_i)$, representing the isometric recruitment curve, cascaded with linear activation dynamics, $h_{LAD,i}(t)$. The multiplicative effect of the joint angle and joint angular velocity on the active torque developed by the muscle is modelled by $F_{m,i}(\phi_i, \dot{\phi}_i)$, and the state-space system corresponding to linear activation dynamics, $h_{LAD,i}(t)$, has continuous-time state-space model matrices $[\boldsymbol{A}_{m,i}, \boldsymbol{B}_{m,i}, \boldsymbol{C}_{m,i}]$ (state, input and output respectively), and states x_i. Writing $\boldsymbol{u} = [0, u_2, 0, 0, u_5]^T$, therefore assume the form

$$\boldsymbol{\tau}(\boldsymbol{u}, \boldsymbol{\Phi}, \dot{\boldsymbol{\Phi}}) = \left[0, \tau_2(u_2, \phi_2, \dot{\phi}_2), 0, 0, \tau_5(u_5, \phi_5, \dot{\phi}_5)\right]^T \quad (2)$$

Within suitable joint ranges there exists a bijective transformation between coordinate sets given by $\boldsymbol{\Phi} = \boldsymbol{k}(\boldsymbol{\Theta})$ so that the Lagrangian equation in one variable can be expressed in terms of the other using the chain rule. Hence a combined model of the support and human arm is given by

$$\boldsymbol{B}(\boldsymbol{\Phi})\ddot{\boldsymbol{\Phi}} + \boldsymbol{C}(\boldsymbol{\Phi}, \dot{\boldsymbol{\Phi}})\dot{\boldsymbol{\Phi}} + \boldsymbol{F}(\boldsymbol{\Phi}, \dot{\boldsymbol{\Phi}}) + \boldsymbol{G}(\boldsymbol{\Phi}) + \boldsymbol{K}(\boldsymbol{\Phi}) = \boldsymbol{\tau}(\boldsymbol{u}, \boldsymbol{\Phi}, \dot{\boldsymbol{\Phi}}) - \boldsymbol{J}_h^T(\boldsymbol{\Phi})\boldsymbol{h} \quad (3)$$

See [12] for full details, including experimental procedures used to identify the parameters appearing in (3).

III. FES CONTROL STRATEGY

A suitable clinical objective is to control the pulsewidth inputs $u_2(t)$ and $u_5(t)$ to assist tracking performance of the supported human arm system such that the outputs $\phi_2(t)$ and $\phi_5(t)$ of the vector $\boldsymbol{\Phi}(t)$ track reference trajectories $\hat{\phi}_2(t)$ and $\hat{\phi}_5(t)$ respectively, whilst the remaining joint angles remain bound-input bounded-output stable.

A. Input/Output linearization

An input/output linearization scheme is developed for the biomechanical arm system, and then combined with a feedback tracking controller and linear model-based ILC. This generalises a previous approach [8], [9] applied clinically, and has potential for application to a broad range of support mechanisms and choice of stimulated muscles.

The linear component of stimulated muscle structures is most often assumed to be second order [11], and hence the general state-space model in controllable canonical form can be written as

$$\dot{x}_i = \underbrace{\begin{bmatrix} -d_{i,1} & -d_{i,2} \\ 1 & 0 \end{bmatrix}}_{\boldsymbol{A}_{m,i}} x_i + \underbrace{\begin{bmatrix} 1 \\ 0 \end{bmatrix}}_{\boldsymbol{B}_{m,i}} h_{IRC,i}(u_i)$$

$$\frac{\tau_i}{F_{m,i}(\phi_i,\dot{\phi}_i)} = \underbrace{\begin{bmatrix} n_{i,1} & n_{i,2} \end{bmatrix}}_{\boldsymbol{C}_{m,i}} x_i \qquad i \in \{2,5\} \quad (4)$$

is assumed for (1), and hence $\mathcal{L}\{h_{LAD,i}(t)\} = \frac{n_{i,1}s+n_{i,2}}{s^2+d_{i,1}s+d_{i,2}}$. Now express the system (3) as

$$\begin{aligned} \dot{\boldsymbol{x}} &= \boldsymbol{f}(\boldsymbol{x}) + \boldsymbol{g}(\boldsymbol{x}) \begin{bmatrix} h_{LAD,2}(u_2) \\ h_{LAD,5}(u_5) \end{bmatrix} \\ \begin{bmatrix} \phi_2 & \phi_5 \end{bmatrix}^T &= \boldsymbol{h}(\boldsymbol{x}) \end{aligned} \quad (5)$$

where $\boldsymbol{x} = [\boldsymbol{\Phi}^T,\ \dot{\boldsymbol{\Phi}}^T,\ x_2^T,\ x_5^T]^T$ and $\boldsymbol{f}(\boldsymbol{x}) =$

$$\begin{bmatrix} \dot{\boldsymbol{\Phi}} \\ p_1(\boldsymbol{\Phi},\dot{\boldsymbol{\Phi}}) \\ p_2(\boldsymbol{\Phi},\dot{\boldsymbol{\Phi}}) + \left(\boldsymbol{B}(\boldsymbol{\Phi})^{-1}\right)_{2,2} F_{m,2}(\phi_2,\dot{\phi}_2)(n_{2,1}x_{2,1} + n_{2,2}x_{2,2}) \\ p_3(\boldsymbol{\Phi},\dot{\boldsymbol{\Phi}}) \\ p_4(\boldsymbol{\Phi},\dot{\boldsymbol{\Phi}}) \\ p_5(\boldsymbol{\Phi},\dot{\boldsymbol{\Phi}}) + \left(\boldsymbol{B}(\boldsymbol{\Phi})^{-1}\right)_{5,5} F_{m,5}(\phi_5,\dot{\phi}_5)(n_{5,1}x_{5,1} + n_{5,2}x_{5,2}) \\ -d_{2,1}x_{2,1} - d_{2,2}x_{2,2} \\ x_{2,1} \\ -d_{5,1}x_{5,1} - d_{5,2}x_{5,2} \\ x_{5,1} \end{bmatrix}$$

where $p_i(\boldsymbol{\Phi},\dot{\boldsymbol{\Phi}}) =$

$$-\left(\boldsymbol{B}(\boldsymbol{\Phi})^{-1}\left(\boldsymbol{C}(\boldsymbol{\Phi},\dot{\boldsymbol{\Phi}})\dot{\boldsymbol{\Phi}} + \boldsymbol{F}(\boldsymbol{\Phi},\dot{\boldsymbol{\Phi}}) + \boldsymbol{G}(\boldsymbol{\Phi}) + \boldsymbol{K}(\boldsymbol{\Phi})\right)\right)_i,$$

$$\boldsymbol{g}(\boldsymbol{x}) = \begin{bmatrix} g_1(\boldsymbol{x})^T \\ g_2(\boldsymbol{x})^T \end{bmatrix}^T = \begin{bmatrix} 0&0&0&0&0&0&0&0&0&0&1&0&0&0 \\ 0&0&0&0&0&0&0&0&0&0&0&0&1&0 \end{bmatrix}^T$$

and $\boldsymbol{h}(\boldsymbol{x}) = \begin{bmatrix} h_1(\boldsymbol{x}) & h_2(\boldsymbol{x}) \end{bmatrix}^T = \begin{bmatrix} \phi_2 & \phi_5 \end{bmatrix}^T$. From [13], for an $m \times m$ system the I/O linearizing controller is

$$\begin{bmatrix} h_{LAD,2}(u_2) \\ h_{LAD,5}(u_5) \end{bmatrix} = \beta(\boldsymbol{x})^{-1}\Big(-\alpha(\boldsymbol{x}) + \boldsymbol{v}\Big) \quad (6)$$

where $\boldsymbol{v}$ is the control input and α and β have components

$$\alpha_i(\boldsymbol{x}) = L_f^{k_i} h_i(\boldsymbol{x}), \qquad \beta_{ij}(\boldsymbol{x}) = L_{g_j} L_f^{k_i-1} h_i(\boldsymbol{x})$$

with $i,\ j = 1,\ldots,m$, and k_i the relative degree of output i. The Lie derivative of $h_i(\boldsymbol{x})$ with respect to $f(\boldsymbol{x})$ and of $h_i(\boldsymbol{x})$ with respect to $g_i(\boldsymbol{x})$ are given by

$$L_f h_i(\boldsymbol{x}) = \frac{\delta h_i}{\delta \boldsymbol{x}} f(\boldsymbol{x}), \qquad L_{g_i} h_i(\boldsymbol{x}) = \frac{\delta h_i}{\delta x} g_i(\boldsymbol{x}) \quad (7)$$

respectively, and $L_f^j h_i(\boldsymbol{x})$ and $L_{g_i} L_f^{j-1} h_i(\boldsymbol{x})$ are given by

$$L_f\left(L_f^{j-1} h_i(\boldsymbol{x})\right), \quad \text{and} \quad L_{g_i}\left(L_f^{j-1} h_i(\boldsymbol{x})\right)$$

respectively. The relative degree k_i, satisfies $L_{g_i} L_f^{k_i-1} h_i(\boldsymbol{x}) \neq 0$, and $L_{g_i} L_f^n h_i(\boldsymbol{x}) = 0$ for $n = 1, 2, \ldots (k_i - 2)$. Assuming $n_{2,1}, n_{5,1} \neq 0$, $k_1, k_2 = 4$, (6) then yields

$$u_2 = h_{\text{IRC},2}^{-1}\left(\frac{\frac{\delta f_7(\boldsymbol{x})}{\delta x} f(\boldsymbol{x}) - v_1}{\left(\boldsymbol{B}(\boldsymbol{\Phi})^{-1}\right)_{2,2} F_{m,2}(\phi_2,\dot{\phi}_2) n_{2,1}}\right) \quad (8)$$

$$u_5 = h_{\text{IRC},5}^{-1}\left(\frac{\frac{\delta f_{10}(\boldsymbol{x})}{\delta x} f(\boldsymbol{x}) - v_2}{\left(\boldsymbol{B}(\boldsymbol{\Phi})^{-1}\right)_{5,5} F_{m,5}(\phi_5,\dot{\phi}_5) n_{5,1}}\right) \quad (9)$$

This leads to the input/output decoupled signals $\phi_2^{(4)} = v_1$, $\phi_5^{(4)} = v_2$ where $\phi_i^{(k)}$ denotes the k^{th} time derivative of ϕ_i.

B. Tracking controller

Trajectory tracking can be achieved using the inputs

$$\begin{aligned} v_1 &= \hat{\phi}_2^{(4)} - a_{13}e_1^{(3)} - a_{12}e_1^{(2)} - a_{11}e_1^{(1)} - a_{10}e_1 \\ v_2 &= \hat{\phi}_5^{(4)} - a_{23}e_2^{(3)} - a_{22}e_2^{(2)} - a_{21}e_2^{(1)} - a_{20}e_2 \end{aligned}$$

where $e_1 = \phi_2 - \hat{\phi}_2$, $e_2 = \phi_5 - \hat{\phi}_5$ are the output error components, and a_{i3}, a_{i2}, a_{i1}, a_{i0} are scalars. Using $\boldsymbol{e} = [e_1, e_2]^T$ and $A_j = \text{diag}\{a_{1j}, a_{2j}\}$ the error dynamics are

$$\underbrace{\begin{bmatrix} \boldsymbol{e}^{(1)} \\ \boldsymbol{e}^{(2)} \\ \boldsymbol{e}^{(3)} \\ \boldsymbol{e}^{(4)} \end{bmatrix}}_{\dot{\boldsymbol{\xi}}} = \underbrace{\begin{bmatrix} 0 & I & 0 & 0 \\ 0 & 0 & I & 0 \\ 0 & 0 & 0 & I \\ -A_0 & -A_1 & -A_2 & -A_3 \end{bmatrix}}_{\boldsymbol{A}} \underbrace{\begin{bmatrix} \boldsymbol{e}^{(0)} \\ \boldsymbol{e}^{(1)} \\ \boldsymbol{e}^{(2)} \\ \boldsymbol{e}^{(3)} \end{bmatrix}}_{\boldsymbol{\xi}} \quad (10)$$

and are stabilised by designing the optimal state feedback $\boldsymbol{v} = -[A_0\ A_1\ A_2\ A_3]\boldsymbol{\xi}$ to minimise

$$J(\boldsymbol{v}) = \int_0^\infty \left(\boldsymbol{\xi}^T Q \boldsymbol{\xi} + \boldsymbol{v}^T R \boldsymbol{v}\right) \quad (11)$$

subject to

$$\dot{\boldsymbol{\xi}} = \begin{bmatrix} 0 & I & 0 & 0 \\ 0 & 0 & I & 0 \\ 0 & 0 & 0 & I \\ 0 & 0 & 0 & 0 \end{bmatrix} \boldsymbol{\xi} + \underbrace{\begin{bmatrix} 0 & 0 & 0 & I \end{bmatrix}^T}_{B} \boldsymbol{v} \quad (12)$$

To provide estimates of the error and derivatives, an observer is implemented for system (12) to minimize the steady-state error covariance, as shown in Fig. 3.

C. Zero Dynamics

A feedback tracking scheme has been implemented for the controlled joints, but stabilisation has not been established for those not controlled by FES. To address this, first express the components of $\boldsymbol{C}(\boldsymbol{\Phi},\dot{\boldsymbol{\Phi}})$ in standard form as

$$c_{i,j} = \sum_{k=1}^{n} c_{i,j,k}\dot{\phi}_k, \quad c_{i,j,k} = \frac{1}{2}\left(\frac{\partial b_{i,j}}{\partial \phi_k} + \frac{\partial b_{i,k}}{\partial \phi_j} - \frac{\partial b_{j,k}}{\partial \phi_i}\right)$$

where $b_{i,j}$ are the components of $\boldsymbol{B}(\boldsymbol{\Phi})$. Now let the indices of the uncontrolled and controlled joint angles be given by the ordered sets $\mathcal{I}_U = \{1,3,4\}$ and $\mathcal{I}_C = \{2,5\}$ respectively. Partition the uncontrolled and controlled joint angles as $\Phi_U = [\phi_{\mathcal{I}_U(1)}, \ldots, \phi_{\mathcal{I}_U(N_U)}]^T$ and $\Phi_C = [\phi_{\mathcal{I}_C(1)}, \ldots, \phi_{\mathcal{I}_C(N_C)}]^T$ respectively, where N_U and N_C are the number of elements in each. Then using $\eta_1 = \Phi_U$, the system (5) and controller (6) yield the system

$$\dot{\boldsymbol{\xi}} = A\boldsymbol{\xi} \quad (13)$$

$$\dot{\boldsymbol{\eta}} = \omega(\boldsymbol{\xi},\eta,t) \quad (14)$$

$$\boldsymbol{e} = \underbrace{\begin{bmatrix} I & 0 & 0 & 0 \end{bmatrix}}_{C} \boldsymbol{\xi} \quad (15)$$

where $\eta = [\eta_1^T,\ \eta_2^T]$, $\omega(\boldsymbol{\xi},\eta,t) =$

$$\begin{pmatrix} \eta_2 \\ -B_U^{-1}(\Phi)\Big(C_U(\Phi,\dot{\Phi})\eta_2 + C_{UC}(\Phi,\dot{\Phi})\Big(\xi_2 + \hat{\Phi}_C^{(1)}\Big) + \\ +F_U(\eta_1,\eta_2) + B_{UC}(\Phi)\Big(\xi_3 + \hat{\Phi}_C^{(2)}\Big)\Big) \end{pmatrix},$$

$\hat{\phi}_C = [\hat{\phi}_2,\ \hat{\phi}_5]^T$, $\Phi = [\eta_1, \xi_1 + \hat{\phi}_C]^T$ and $\dot{\Phi} = [\eta_2, \xi_2 + \hat{\phi}_C^{(1)}]^T$. The design of the support structure is such that the spring term approximately cancels the gravity term, and hence it has been assumed $G_U(\cdot) = -K_U(\cdot)$. The terms $C_U(\Phi, \dot{\Phi})$ and $C_{UC}(\Phi, \dot{\Phi})$ respectively have elements

$$C_{U,i,j} = \sum_{k=1}^{n} c_{\mathcal{I}_U(i),\mathcal{I}_U(j),k}\dot{\phi}_k,\ C_{UC,i,j} = \sum_{k=1}^{n} c_{\mathcal{I}_U(i),\mathcal{I}_C(j),k}\dot{\phi}_k$$

and likewise $B_U(\Phi)$ and $B_{UC}(\Phi)$ have elements

$$B_{U,i,j} = b_{\mathcal{I}_U(i),\mathcal{I}_U(j)},\ B_{UC,i,j} = b_{\mathcal{I}_U(i),\mathcal{I}_C(j)} \tag{16}$$

$F_U(\Phi_U, \dot{\Phi}_U)$ has elements $F_{U,i}$ which take the form

$$\begin{aligned} F_{\mathcal{I}_U(i)}(\phi_{\mathcal{I}_U(i)}, \dot{\phi}_{\mathcal{I}_U(i)}) &= F_{s,\mathcal{I}_U(i)}(\phi_{\mathcal{I}_U(i)}) + F_{v,\mathcal{I}_U(i)}(\dot{\phi}_{\mathcal{I}_U(i)}) \\ &:= F_s(\Phi_U) + F_v(\dot{\Phi}_U) \end{aligned} \tag{17}$$

where $F_s(\cdot)$ and $F_v(\cdot)$ are joint angle and angular velocity dependent friction components respectively. From (13) and (14) the surface $\boldsymbol{\xi} = \mathbf{0}$ defines the integral manifold

$$\dot{\eta} = \omega(0, \eta, t) \tag{18}$$

Since A is stable this system is globally attractive and defines the zero dynamics [13] relative to the output $\boldsymbol{e} = \phi_C - \hat{\phi}_C$.

Theorem 1. Suppose that $\omega(0, \eta_1^*, t) = 0$ for $t \geq 0$, i.e. $(0, \eta_1^*)$ is an equilibrium of the full system (13) - (15), and η_1^* is an equilibrium of the zero dynamics (18), and that A is stable. Then $(0, \eta_1^*)$ of the full system (13) - (15) is locally stable if η_1^* is locally stable for the zero dynamics (18).

Proof. This uses the Center Manifold Theorem, see [13]. □

Stability of the complete system (5) is hence assured if both the actuated and unactuated subsystems are independently stable. The former is guaranteed by the linearizing controller, and the following theorem ensures the latter.

Theorem 2. A sufficient condition for the zero dynamics to be stable is that the function $F_s(\cdot)$ is passive, that is

$$F_{s,i}(\phi_i)\phi_i \geq 0, \qquad i \in \mathcal{I}_U \tag{19}$$

and the function $F_v(\cdot)$ satisfies the sector bound

$$F_{v,i}(\dot{\phi}) \begin{cases} > \bar{F}_{v,i}\dot{\phi}_i & \text{if } \dot{\phi} > 0, \\ < \bar{F}_{v,i}\dot{\phi}_i & \text{otherwise.} \end{cases} \tag{20}$$

where

$$\bar{F}_{v,i} = \sum_{i \neq j} \left| \sum_{k=1}^{N_C} c_{\mathcal{I}_U(i),\mathcal{I}_C(k),\mathcal{I}_U(j)} \hat{\phi}_{\mathcal{I}_C(k)}^{(1)} \right| \qquad i, j \in \mathcal{I}_U \tag{21}$$

Proof. The unactuated system dynamics are given by

$$B_U(\Phi)\ddot{\Phi}_U + C_U(\Phi, \dot{\Phi})\dot{\Phi}_U + C_{UC}(\Phi, \dot{\Phi})\dot{\Phi}_C + F_U(\Phi, \dot{\Phi}) + B_{UC}(\Phi)\ddot{\Phi}_C = 0 \tag{22}$$

The term C_{UC} can be partitioned as $C_{UC}(\Phi, \dot{\Phi}) = \overline{C}_{UC}(\Phi, \dot{\Phi}_C) + \underline{C}_{UC}(\Phi, \dot{\Phi}_U)$, with respective elements

$$\overline{C}_{UC,i,j} = \sum_{k=1}^{N_C} c_{\mathcal{I}_U(i),\mathcal{I}_C(j),\mathcal{I}_C(k)}\dot{\phi}_{\mathcal{I}_C(k)}$$

and $$\underline{C}_{UC,i,j} = \sum_{k=1}^{N_U} c_{\mathcal{I}_U(i),\mathcal{I}_C(j),\mathcal{I}_U(k)}\dot{\phi}_{\mathcal{I}_U(k)}$$

The term $\underline{C}_{UC}(\boldsymbol{\Phi}, \dot{\boldsymbol{\Phi}}_U)\dot{\boldsymbol{\Phi}}_C$ can be written as $\underline{C}_U(\boldsymbol{\Phi}, \dot{\boldsymbol{\Phi}}_C)\dot{\boldsymbol{\Phi}}_U$ where $\underline{C}_U$ has components

$$\underline{C}_{U,i,j} = \sum_{k=1}^{N_C} c_{\mathcal{I}_U(i),\mathcal{I}_C(k),\mathcal{I}_U(j)}\dot{\phi}_{\mathcal{I}_C(k)}$$

This enables us to rewrite system (22) using the substitutions $C_{UC} \Leftrightarrow \overline{C}_{UC}$ and $C_U \Leftrightarrow \overline{C}_U$. Here $\overline{C}_U = C_U + \underline{C}_U$ to give

$$\begin{aligned} B_U(\Phi)\ddot{\Phi}_U + \overline{C}_U(\Phi, \dot{\Phi})\dot{\Phi}_U + \overline{C}_{UC}(\Phi, \dot{\Phi}_C)\dot{\Phi}_C \\ + F_U(\Phi, \dot{\Phi}) + B_{UC}(\Phi)\ddot{\Phi}_C = 0 \end{aligned}$$

When $\boldsymbol{\xi} = \mathbf{0}$ the zero dynamics correspond to

$$\begin{aligned} B_U(\eta_1)\dot{\eta}_2 + \overline{C}_U(\eta_1, \eta_2)\eta_2 + \overline{C}_{UC}(\eta_1)\hat{\phi}_C^{(1)} \\ + F_U(\eta_1, \eta_2) + B_{UC}(\eta_1)\hat{\phi}_C^{(2)} = 0 \end{aligned}$$

This is written as $\dot{\eta}_2 = -h(\eta_1, \eta_2) - g(\eta_1)$ where

$$\begin{aligned} h(\eta_1, \eta_2) &= B_U(\eta_1)^{-1}(\overline{C}_U(\eta_1, \eta_2)\eta_2 + F_s(\eta_1) + F_v(\eta_2)) \\ g(\eta_1) &= B_U(\eta_1)^{-1}(\overline{C}_{UC}(\eta_1)\hat{\Phi}_C^{(1)} + B_{UC}(\eta_1)\hat{\Phi}_C^{(2)}) \end{aligned}$$

The equilibrium point satisfies $h(\eta_1^*, 0) + g(\eta_1^*) = 0$, and, from [14], the system can be interpreted as the conservative system $\dot{\eta}_2 + g(\tilde{\eta}_1) = 0$ acted upon by an external force $-h(\tilde{\eta}_1, \eta_2)$ where $\tilde{\eta}_1 = \eta_1 - \eta_1^*$. Accordingly, introduce the potential energy function $V(\tilde{\eta}_1, \eta_2) =$

$$\eta_2^T \frac{B_U}{2}(\tilde{\eta}_1)\eta_2 + \int_0^{\tilde{\eta}_1} F_s(\sigma)\delta\sigma + \int_0^{\tilde{\eta}_1} \overline{C}_{UC}(\sigma)\hat{\Phi}_C^{(1)} + B_{UC}(\sigma)\hat{\Phi}_C^{(2)}\delta\sigma$$

The first term corresponds to the kinetic energy in the unactuated joint system, and the second corresponds to its potential energy and is positive definite via (19). The third is the potential energy transferred from the actuated joints which is assumed to be bounded in a finite time. Under the influence of the external force $-h(\tilde{\eta}_1, \eta_2)$, the rate of supply of external energy to the unactuated system is $\dot{V}(\tilde{\eta}_1, \eta_2) =$

$$\begin{aligned} &\eta_2^T B_U(\tilde{\eta}_1)\dot{\eta}_2 + \eta_2^T \frac{\dot{B}_U(\tilde{\eta}_1)}{2}\eta_2 + \eta_2^T F_s(\tilde{\eta}_1) + \eta_2^T\Big(\bar{C}_{UC}(\tilde{\eta}_1)\hat{\Phi}_C^{(1)} \\ &+ B_{UC}(\tilde{\eta}_1)\hat{\Phi}_C^{(2)}\Big) = \eta_2^T\left(\frac{\dot{B}_U(\tilde{\eta}_1)}{2} - \overline{C}_U(\tilde{\eta}_1, \eta_2)\right)\eta_2 - \eta_2^T F_v(\eta_2) \\ &\leq \eta_2^T\left(\frac{1}{2}\dot{B}_U(\tilde{\eta}_1) - \overline{C}_U(\tilde{\eta}_1, \eta_2) - \bar{F}_v\right)\eta_2 \end{aligned}$$

for stability. This is equivalent to the requirement

$$\min_i \Re\left(\lambda_i\left(\frac{\dot{B}_U(\tilde{\eta}_1)}{2} - C_U(\tilde{\eta}_1, \eta_2) - \underline{C}_U(\tilde{\eta}_1, \eta_2) - \bar{F}_v\right)\right) < 0$$

As $\frac{1}{2}\dot{B}_U(\eta_1) - C_U(\tilde{\eta}_1, \eta_2)$ is skew-symmetric, a sufficient condition is that $\underline{C}_U(\tilde{\eta}_1, \eta_2) + \bar{F}_v$ is diagonally dominant with positive diagonal entries, which is satisfied by (20). □

Condition (21) can always be met by adding damping to the unactuated joints. From (21) bounds on F_v scale with $\hat{\Phi}_C^{(1)}$, and hence (19) and (20) are relaxed if $|\hat{\Phi}_C^{(1)}|$ is small.

D. Error Estimation

The linearizing controller inputs (8) and (9) require the system states, which comprise the system joint angles and angular velocities, together with the muscle states x_2, x_5. The latter cannot be read directly but can be estimated using

another observer around the arm system. Each channel is designed for system (4) with input $h_{IRC,i}(u_i)$ and output

$$F_{m,i}(\phi_i,\dot{\phi}_i)^{-1}\left(\boldsymbol{B}(\boldsymbol{\Phi})^{-1}\right)_{i,i}\left(\ddot{\phi}_i - p_i(\boldsymbol{\Phi},\dot{\boldsymbol{\Phi}})\right),\quad i\in\{2,5\}$$

These provide the estimates $\hat{\boldsymbol{x}}_i$ shown in Fig. 3.

E. Linear model-based ILC

ILC is a methodology applicable to systems which repeatedly track a fixed reference signal over a finite time interval, termed a trial. After each trial the system is reset to the same initial conditions, and within this resetting period data from the previous trial is used to modify the control input in order to reduce the error in the subsequent trial. ILC is often applied in combination with a feedback controller to ensure stabilisation, disturbance rejection, and baseline tracking performance. A robust ILC scheme can mitigate against significant dynamic changes and model inaccuracy, and in the current application the voluntary effort of the patient can also be treated as an iteration-invariant disturbance. There are many available update procedures (see [15] for an overview of the literature), the most common form of which is shown in Fig. 3, where the subscript k denotes the k^{th} trial, and f_k is the ILC feedforward signal. The ILC update f_{k+1} (shown in the dashed box) is determined off-line between trials, through use of the learning filter $L(s)$ and a robustness filter $Q(s)$.

The transfer-function from error to the feedforward control input f_k is the negative process sensitivity $-S_p$

$$e_k = \underbrace{C(sI-A)^{-1}B}_{-S_p} f_k \tag{23}$$

with components given by (10), (12) and (15), and hence the ILC design collapses to the design of two independent SISO controllers with both Q and L diagonal matrices. Using the ILC learning update

$$f_{k+1} = Q\left(f_k + Le_k\right) \tag{24}$$

the relation between e_{k+1} and e_k results in $e_{k+1} = Q\left(1 - S_pL\right)e_k$, with convergence criteria

$$\left|Q\left(1-S_pL\right)\right| < 1, \qquad \forall\omega \tag{25}$$

The learning filter $L(s)$ is designed to approximate the process sensitivity at low frequencies to result in accurate tracking, and Q takes the form of a lowpass filter to provide robustness to modeling errors and non-repetitive signals at high frequencies. For the design of the learning filter a Zero Phase Error Tracking Controller (ZPETC) is used [16].

IV. EXPERIMENTAL RESULTS

A. Trajectory Selection

During treatment 9 trajectories were generated for each patient that corresponding to lifting and extending the upper arm and forearm over a period of 5 or 10 seconds. Corresponding references $\hat{\phi}_2$ and $\hat{\phi}_5$ were calculated, with variation in the uncontrolled variables permissible since only ϕ_2 and ϕ_5 are controlled. Following ethical approval, the control scheme was first experimentally implemented on unimpaired participants and representative results from this group are given in the next subsection. The experiments use sampling frequencies of 1000Hz and 40Hz for capturing and computation of control signals respectively.

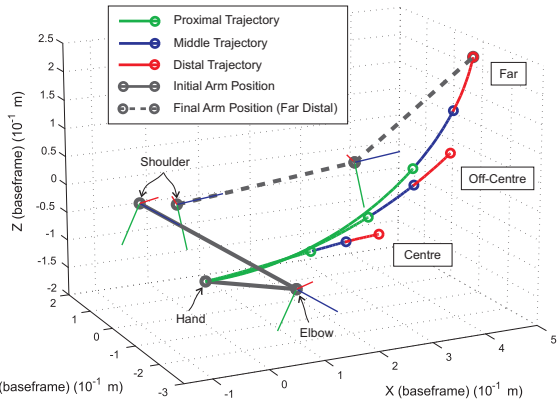

Fig. 4. Reference trajectories corresponding to arm extension.

B. Experimental Test Procedure and Results

Each unimpaired participant was seated in the system, which was adjusted to their individual arm dimensions. The level of support was adjusted so that their arm was raised 5cm above their lap. Surface electrodes were placed on the anterior deltoid and triceps muscles and adjusted to elicit the maximum appropriate movement. Each FES channel comprises a sequence of bi-phasic pulses at 40Hz, whose pulsewidth is the controlled variable. The identification procedure described in [12] was then conducted. In clinical trials, VR software displays the reference to the patient, however during testing with unimpaired subjects they were not shown the tasks and were instructed to apply no voluntary effort. After each trial their arm was repositioned at the start position.

Tracking results for the joints ϕ_2 and ϕ_5 are shown in Fig. 5, together with the applied stimulation pulsewidth signals u_1 and u_2. Corresponding error norm results are shown in Fig. 6. Optimal weights used in (11) were $Q = I$ and $R = 0.01$. The cut-off frequency used in the ZPETC design was 10 Hz.

The results confirm error convergence to low levels in a small number of trials, and an input signal which is within comfortable limits for the participant. Note that the decrease in tracking accuracy at the conclusion of the trial can be addressed by increasing the trial duration and holding the reference at its end value.

V. CONCLUSIONS AND FUTURE WORK

A combined input/output linearization and ILC approach has been developed to provide upper arm trajectory tracking using FES. Building on control structures that have a proven track record in upper limb stroke rehabilitation, the proposed control scheme significantly extends the scope of current ILC approaches in this area since it explicitly incorporates the unactuated joints and ensures stability of the overall system.

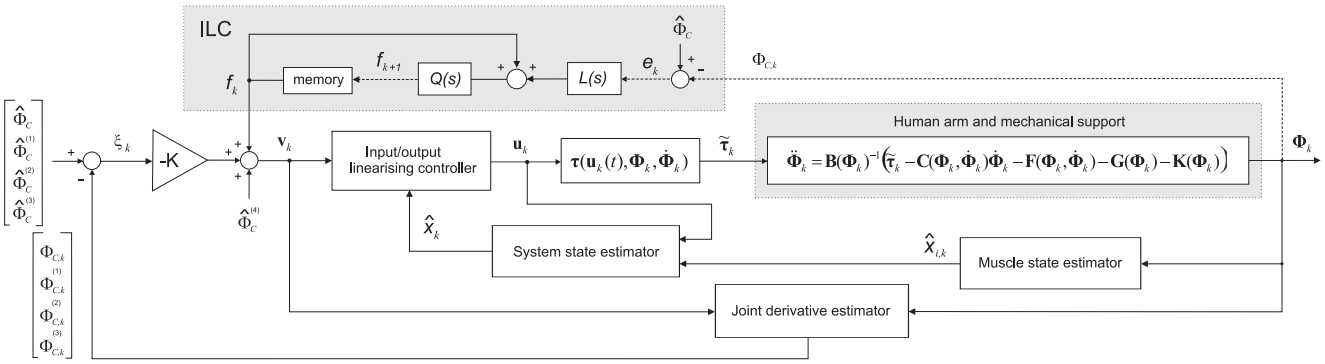

Fig. 3. I/O linearizing/decoupling control scheme with stabilising feedback and linear ILC.

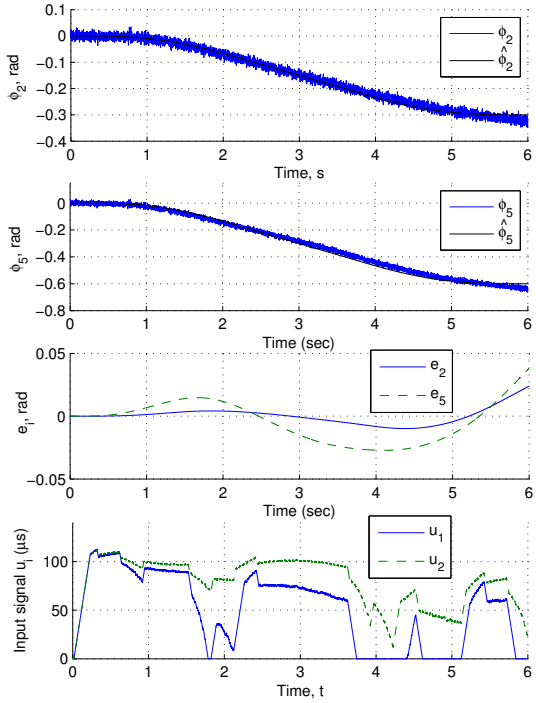

Fig. 5. Trial $k = 10$ signals using Zero Phase Error Tracking Controller.

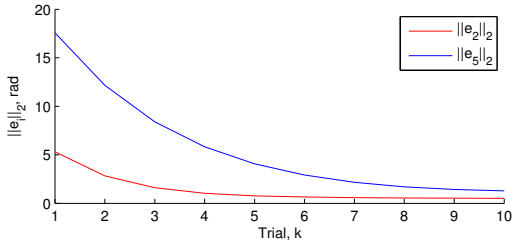

Fig. 6. Error norm results using Zero Phase Error Tracking Controller.

Moreover, the controller is suitable for general application across a broad range of support structures and stimulated muscle sets. It will be used in clinical trials to enable increased patient comfort, tracking accuracy and hence potential for rehabilitation.

REFERENCES

[1] S. Barrreca, S. L. Wolf, S. Fasoli, and R. Bohannon, "Treatment interventions for the paretic upper limb of stroke survivors: A critical review," *Neurorehab. Neural Re.*, vol. 17, no. 4, pp. 220–226, 2003.

[2] J. Mehrholz, T. Platz, J. Kugler, and M. Pohl, "Electromechanical and robot-assisted arm training for improving arm function and activities of daily living after stroke," *Cochrane Db Syst Rev*, vol. 4, no. CD006876, 2008.

[3] P. Langhorne, F. Coupar, and A. Pollock, "Motor recovery after stroke: a systematic review," *Lancet Neurol*, vol. 8, no. 8, pp. 741–54, 2009.

[4] D. N. Rushton, "Functional electrical stimulation and rehabilitation - an hypothesis," *Med. Eng. Phys.*, vol. 25, no. 1, pp. 75–78, 2003.

[5] C. L. Lynch and M. R. Popovic, "Functional electrical stimulation: Closed-loop control of induced muscle contractions," *IEEE Control Syst. Mag.*, vol. 28, no. 2, pp. 40–50, 2008.

[6] J. G. Hincapie and R. F. Kirsch, "Feasibility of EMG-based neural network controller for an upper extremity neuroprosthesis," *IEEE Trans. Neural Syst. Rehabil. Eng.*, vol. 17, no. 1, pp. 80–90, 2009.

[7] C. T. Freeman, E. Rogers, A. M. Hughes, J. H. Burridge, and K. L. Meadmore, "Iterative learning control in healthcare: Electrical stimulation and robotic-assisted upper limb stroke rehabilitation," *IEEE Control Systems Magazine*, vol. 32, no. 1, pp. 18–43, 2012.

[8] C. T. Freeman, A. M. Hughes, J. H. Burridge, P. H. Chappell, P. L. Lewin, and E. Rogers, "Iterative learning control of FES applied to the upper extremity for rehabilitation," *Control Eng. Pract.*, vol. 17, no. 3, pp. 368–381, March 2009.

[9] A. M. Hughes, C. T. Freeman, J. H. Burridge, P. H. Chappell, P. Lewin, and E. Rogers, "Feasibility of iterative learning control mediated by functional electrical stimulation for reaching after stroke," *Neurorehab. Neural Re.*, vol. 23, no. 6, pp. 559–568, 2009.

[10] P. S. Lum, C. G. Burgar, and P. C. Shor, "Evidence for improved muscle activation patterns after retraining of reaching movements with the mime robotic system in subjects with post-stroke hemiparesis," *IEEE Trans. Neural Syst. Rehabil. Eng.*, vol. 12, no. 2, pp. 186–194, 2004.

[11] F. Le, I. Markovsky, C. T. Freeman, and E. Rogers, "Identification of electrically stimulated muscle models of stroke patients," *Control Eng. Pract.*, vol. 18, pp. 396–407, 2010.

[12] C. T. Freeman, D. Tong, K. Meadmore, Z. Cai, E. Rogers, A. M. Hughes, and J. H. Burridge, "Phase-lead iterative learning control algorithms for functional electrical stimulation based stroke rehabilitation," *Proc. Inst. Mech. Eng. I-J. Syst. Cont. Eng.*, vol. 225, no. 6, pp. 850–859, 2011.

[13] A. Isidori, *Nonlinear Control Systems*, 2nd ed. Berlin: Springer-Verlag, 1989.

[14] D. W. Jordan and P. Smith, *Nonlinear Ordinary Differential Equations, an introduction to dynamical systems*. Oxford University Press, 2006.

[15] D. A. Bristow, M. Tharayil, and A. G. Alleyne, "A survey of iterative learning control, a learning-based method for high-performance tracking control," *IEEE Control Syst. Mag.*, vol. 26, no. 3, pp. 96–114, 2006.

[16] M. Tomizuka, "Zero phase error tracking algorithm for digital control," *J. Dyn. Syst. -T ASME*, vol. 109, pp. 65–68, March 1987.